Available online at www.sciencedirect.com
ScienceDirect
Journal of Power Sources 158 (2006) 1012–1018
JOURNAL OF POWER SOURCES
www.elsevier.com/locate/jpowsour

Investigation of the high-frequency resistance of a lead-acid battery

F. Huet [a,*], R.P. Nogueira [a], P. Lailler [b], L. Torcheux [b]

[a] *UPR15 du CNRS, Interfaces et Systèmes Electrochimiques, Université Pierre et Marie Curie, Case Courrier 133, 4 Place Jussieu, 75252 Paris Cedex 05, France*
[b] *EXIDE Technologies, CEAC, 5/7 Allée des Pierres Mayettes, 92636 Gennevilliers Cedex, France*

Available online 27 December 2005

Abstract

The high-frequency resistance, R_{HF}, or internal resistance, of 45 Ah flooded tubular lead-acid battery (LAB) cells was monitored during cycling at constant rates between *C*/100 and *C*/10 in order to understand the origin of the R_{HF} variations and to evaluate the feasibility of monitoring the state-of-charge (SOC) with this parameter. It is shown that the R_{HF} variations did not depend on the electrolyte-conductivity variations, as usually indicated in the literature. At a low discharging rate (*C*/100), R_{HF} increased only at low SOCs, with a high final value, while at a high rate (*C*/10) R_{HF} increased progressively from the beginning of the discharge, with a low final value. This has been interpreted as the consequence of the shape and size of the $PbSO_4$ crystals in the pores of the active material, which are the result of the continuous competition between crystal nucleation and crystal growth. R_{HF} informs on the structure of the $PbSO_4$ layer, and therefore, depends strongly on the history of the previous cyclings of the cell. Monitoring the SOC from the single value of R_{HF} was found to be impossible since, for different cycling rates, distinct values of SOC may correspond to the same value of R_{HF}. Fluctuations of R_{HF} were also measured at different SOC: they allow detection of gas evolution in the cell and could provide complementary information for estimating the SOC of LABs.

Keywords: Lead-acid battery; State-of-charge; High-frequency resistance; Internal resistance; Electrochemical impedance; Electrochemical noise

1. Introduction

The need of a reliable real-time method for estimating the state of health (SOH) or state-of-charge (SOC) of lead-acid batteries (LAB) has accompanied their development in the last decades [1,2]. Particularly, the possibility of using an electrochemical parameter as a reliable gauge for monitoring both the SOC and SOH has been the matter of several studies [3–7]. Nevertheless, no definitive method has been undoubtedly validated and the quest of an accurate and easily implemented SOH and/or SOC indicator remains a subject of great interest [8]. Many studies were based upon the electrochemical impedance technique that provides a complete description of the dynamic behaviour of a metal–electrolyte interface from the low-frequency limit (steady state) to the purely resistive high-frequency limit. The high-frequency resistance, R_{HF}, of a LAB cell (also called internal resistance and related to the conductance $1/R_{HF}$) has been found to give distinct values for fully charged and fully discharged LAB cells and was then proposed as a potentially interesting parameter for SOC- and SOH-monitoring [9–11].

In the present work, the evolution of the high-frequency resistance of a LAB cell of 45 Ah capacity has been investigated during the charge and discharge of the cell at various rates in order to determine the origin of the R_{HF} variations and verify the feasibility of SOC or SOH diagnosis based on the measurement of the mean value of R_{HF} and of a parameter characterizing its time fluctuations. The influence of the temperature and conductivity of the bulk electrolyte on the R_{HF} evolution is also discussed.

2. Experimental

Tubular 2 V LAB cells of 45 Ah capacity from CEAC-Exide were studied in the present work. The electrochemical impedance measurements were performed using a white noise as excitation signal. The overall LAB impedance was measured from the voltage, *V*, at the terminals of the cell and the impedances of the positive and negative plates were obtained from their potential, V_{pos} and V_{neg}, respectively, measured

* Corresponding author. Tel.: +33 1 4427 4136; fax: +33 1 4427 4074.
E-mail address: frh@ccr.jussieu.fr (F. Huet).

0378-7753/$ – see front matter © 2005 Elsevier B.V. All rights reserved.
doi:10.1016/j.jpowsour.2005.11.026

against a saturated mercurous sulphate reference electrode (ESS) immersed above the plates.

The real-time measurement of the high-frequency resistance R_{HF} was possible thanks to a specific apparatus developed at the UPR15 CNRS that delivered a real-time analog signal proportional to the R_{HF} value. This signal was the system response to a single high-frequency (1.8 kHz) current perturbation defined in preliminary impedance measurements so as to ensure that the cell impedance was actually close to the R_{HF} value during the whole charge or discharge. The complete experimental set-up has been described in Ref. [12] in which the R_{HF} evolution with the SOC was investigated for a 1200 Ah LAB cell charged and discharged at a single rate (C/120).

Several charge and discharge rates were employed under galvanostatic control by means of a galvanostat specially conceived to deliver currents of high amplitude (up to 10 A), including in the dynamic regime, which were necessary for cycling the cells at high rates and measure small impedance values (in the range of mΩ). All experiments were carried out at room temperature without specific temperature control.

3. Results and discussion

In a first set of experiments, the overall electrochemical impedance of the cell and the impedances of the negative and positive plates were measured in order to determine the characteristic frequency, F_{HF}, at which the R_{HF} value should be measured. F_{HF} corresponds to the frequency at which the impedance diagram in the Nyquist plot intercepts the real axis at high frequency, as explained in Fig. 1 that shows that the impedance diagram of the cell strongly depends on the charging (Fig. 1A) or discharging (Fig. 1B) regime, except at high frequency. This indicates that the high-frequency resistance R_{HF} measured at a given time, that is, at a given SOC, does not depend on the dc current at which it is measured. In Fig. 1, the high values of R_{HF} (7.5 mΩ) were due to bad connections at the cell terminals, which is a measurement artefact often encountered with impedance values in the mΩ range. The problem was fixed by a proper choice of the connectors and the impedance measurements were validated when the overall impedance of the cell was found to be equal to the sum of the impedances of the positive and negative plates at any frequency. Fig. 2 illustrates the results obtained for the positive and negative plates. A small difference appeared in the R_{HF} values of the positive plate in fully charged or fully discharged conditions, regardless the discharge rate. On the contrary, the negative plate showed significant differences: compared to the fully charged condition, the R_{HF} value at the end of the discharge increased by approximately 35% (from ≈2 mΩ to 2.7 mΩ at C/10) or 150% (from ≈2 mΩ to 5 mΩ at C/100). This indicates that the overall LAB behaviour was mostly controlled by the negative plate, which was confirmed by the evolution profile of the potentials V, V_{pos}, and V_{neg} depicted in Fig. 3. Indeed, the V and V_{neg} curves are quite "parallel", showing that the general battery performance was limited by the negative plate. In that experiment, the cell was fully discharged before delivering a capacity of 45 Ah because the previous charge was not complete.

The LAB cells have then been submitted to several cycles of charge and discharge at different rates (C/10, C/20, C/65, and C/100). Table 1 summarizes the mean values obtained for R_{HF} and F_{HF} in the different conditions. It can be seen that both parameters show increasing values when the cell is discharged and that the final values are higher for the slowest discharge rates. In a first glance, this indicates that in addition to R_{HF}, F_{HF} could also be a parameter allowing the SOC or SOH diagnosis. It is worth noticing, however, that the F_{HF} values show a stronger dispersion, illustrated in Table 1 by the high values of the relative error obtained, which seems to hinder the usefulness of this parameter at least in the experimental conditions of this study, in spite of promising results found by other authors [13].

As for the overall impedance and the cell potential, the R_{HF} and F_{HF} mean values were mostly controlled by the negative plates, as seen in Tables 2 and 3 for the positive and negative plates, respectively. It must be noticed that the sum of the R_{HF} values of the positive and negative plates does not necessarily correspond to the R_{HF} value of the cell because the three values are not measured at the same frequency and also because the values given in Tables 2 and 3 are values averaged from several experiments on the LAB cells. Small and not monotonic variations of R_{HF} and F_{HF} were measured for the positive plates, while a clear increase of the values, similar to that in Table 1,

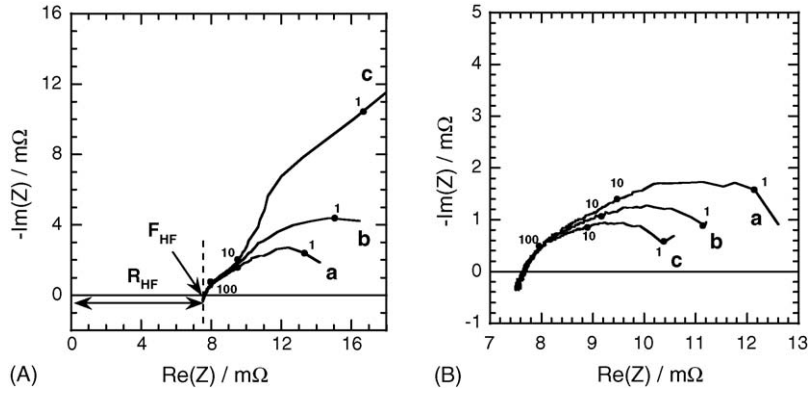

Fig. 1. Electrochemical impedance diagrams of the discharged 45 Ah LAB cell measured at different charge (A) or discharge (B) rates: (a) C/100; (b) C/20; (c) C/10 (frequencies in Hz).

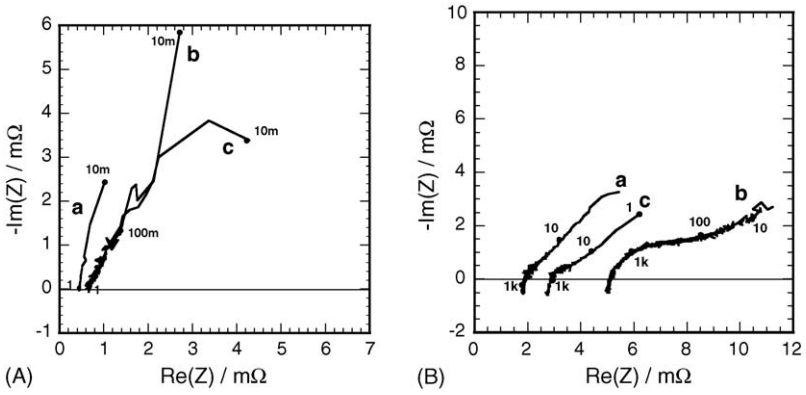

Fig. 2. Electrochemical impedance diagrams of the positive (A) and negative (B) plates of the 45 Ah LAB cell at different conditions: (a) fully charged at a *C*/100 rate; (b) fully discharged at a *C*/100 rate; (c) fully discharged at a *C*/10 rate (frequencies in Hz).

was observed for the negative plates. Here again, a strong dispersion of the F_{HF} values seems to compromise the reliability of this parameter as a SOC or SOH indicator. Subsequent measurements were then limited to the real-time evolution of R_{HF} during different charge and discharge cycles.

The fact that the F_{HF} values increased during the cell discharge was taking into account when the frequency of the current excitation employed in the real-time R_{HF}-monitoring was chosen. The value retained (1.8 kHz) was close to that of F_{HF} for the discharged cells but was slightly different of F_{HF} in full-charge conditions (see Table 1), which gave an error on the R_{HF} value estimated to be equal to 8% in that case.

The time evolution of R_{HF} during discharges at different rates depicted in Fig. 4 clearly depends on the discharge rate, while R_{HF} did not depend on the dc current at which it was measured, as shown above. The initial values of R_{HF} show a certain scatter because the previous charges had not been performed at the same rate. At the first stage of the discharge there is a fast decrease of R_{HF} (of small amplitude at the slowest discharge rate of *C*/100), the explanation of which is not yet understood, followed by an increase leading to different final values similar to those given in Table 1. The shape of the curve, as well as the final R_{HF} value, is strongly dependent on the discharge rate, which seems to preclude or seriously hinder a SOC-monitoring based on the single value of R_{HF}, in applications in which the actual discharge profiles are prone to be irregular and unpredictable. Moreover, at low discharge rates most of the R_{HF} change occurs in the last stage of the discharge, as already observed for a 1200 Ah LAB cell dis-

Table 1
Mean values and relative errors of R_{HF} and F_{HF} of 45 Ah LAB cells fully charged at a *C*/10 rate and fully discharged at different rates

Overall LAB	Charged, *C*/10	Discharged, *C*/10	Discharged, *C*/20	Discharged, *C*/65	Discharged, *C*/100
$\langle R_{HF}\rangle$ (mΩ)	2.50	3.42	3.63	4.74	5.68
Error (%)	11.2	8.5	6.1	3.4	16.2
$\langle F_{HF}\rangle$ (kHz)	0.52	0.91	1.43	1.87	2.20
Error (%)	32.7	34.1	23.1	63.1	27.3

Table 2
Mean values and relative errors of $R_{HF,pos}$ and $F_{HF,pos}$ of LAB-positive plates fully charged at a *C*/10 rate and fully discharged at different rates

Positive plate	Charged, *C*/10	Discharged, *C*/10	Discharged, *C*/20	Discharged, *C*/65	Discharged, *C*/100
$\langle R_{HF}\rangle$ (mΩ)	0.42	0.52	0.43	0.96	0.71
Error (%)	57.1	67.3	58.1	30.2	46.5
$\langle F_{HF}\rangle$ (Hz)	16.9	20.4	31.7	54.0	53.5
Error (%)	41.0	57.3	58.0	94.3	46.7

Table 3
Mean values and relative errors of $R_{HF,neg}$ and $F_{HF,neg}$ of LAB-negative plates fully charged at a *C*/10 rate and fully discharged at different rates

Negative plate	Charged, *C*/10	Discharged, *C*/10	Discharged, *C*/20	Discharged, *C*/65	Discharged, *C*/100
$\langle R_{HF}\rangle$ (mΩ)	1.93	2.71	2.75	3.34	4.99
Error (%)	9.8	12.5	13.4	6.0	13.0
$\langle F_{HF}\rangle$ (kHz)	1.15	1.29	2.62	3.62	3.36
Error (%)	48.7	37.2	36.2	1.0	15.2

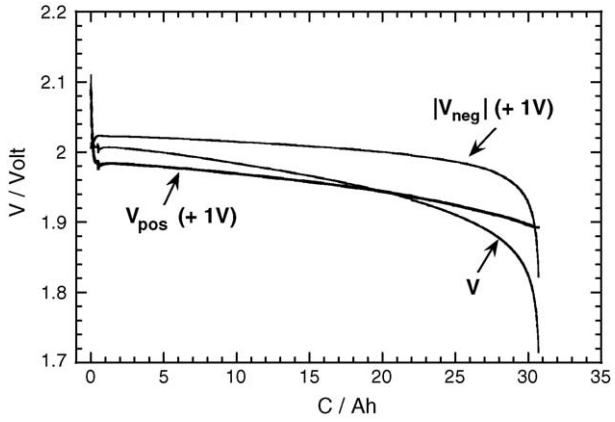

Fig. 3. Evolution of the overall potential of the LAB cell, V, and of the negative and positive plates, V_{neg} and V_{pos}, during a $C/20$ discharge. The potentials of the positive and negative plates have been shifted vertically by 1 V.

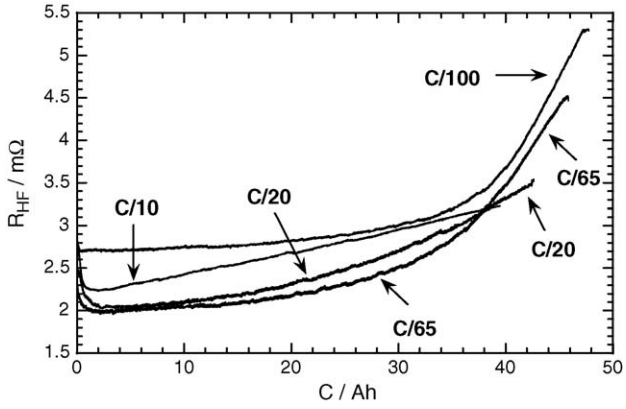

Fig. 4. Evolution of R_{HF} during the discharge of the LAB cell at different discharge rates.

charged at a $C/120$ rate [12]. The increase in the R_{HF} values must be ascribed to the progressive screening of the active material by insulating $PbSO_4$ crystals. The fact that the size and shape of the crystals depend on the discharge current explains the difference in the curves presented in Fig. 4. Indeed, at high currents the higher nucleation rate of $PbSO_4$ nuclei leads to numerous and small $PbSO_4$ crystals that block the pores of the active material quicker, but less completely, than the well-structured crystals formed at low currents. This explains the faster increase of R_{HF} at $C/10$ and $C/20$ and the final low R_{HF} value. At lower currents ($C/65$ and $C/100$), R_{HF} changed slightly during almost 75% of the discharge before increasing rapidly and strongly when the last accessible areas of active material became blocked by the growth of the well-structured crystals. This is corroborated by the results presented in Fig. 5 that gives the V and R_{HF} profiles obtained during a two-step discharge ($C/20$ followed by $C/100$ after a 24 h rest delay). The two potential drops indicate the end of each discharge cycle. The final R_{HF} value is lower than that obtained for a single-step $C/100$ discharge, showing that the active material had been made unavailable in great part by the rapid growth of small crystals during the $C/20$ discharge.

It is also worth noticing that the R_{HF} value was almost constant during the 24 h rest, which is an indication that the R_{HF} variation cannot be explained by the increase in the electrolyte resistivity in the pores of the electrodes since the 24 h rest should be long enough to homogenize the electrolyte concentration. To evaluate the influence of the bulk-electrolyte resistivity, ρ, on R_{HF}, a conductivity cell was immersed above the plates and ρ was measured at different stages of a $C/100$ discharge. The comparative evolution of ρ and R_{HF}, which was not continuously measured in that experiment, is depicted in Fig. 6 that clearly points out the independence of the variations of R_{HF} and ρ, which vary in opposite directions during the discharge. The total charge delivered was only 25 Ah because the cell had been accidentally overdischarged during several hours. Despite an overcharge of at least 40 Ah, the cell could not retrieve its nominal capacity of 45 Ah. The decrease in the ρ values during the discharge seems to be related to the fact that the electrical conductivity of the sulphuric acid is not monotonically dependent on its concentration, reaching a maximum at about 30% of mass fraction; in the fully charged condition, the acid mass fraction was probably higher than that corresponding to the maximum conductivity. This reinforces the interpretation of the dependence of R_{HF} upon the formation of insulating $PbSO_4$ crystals of different shape and size according to the charge/discharge profile, mainly on the negative plate according to Tables 2 and 3. This result is in agreement with the fact that the value of R_{HF} remained unchanged when the exhausted electrolyte of a fully discharged cell was replaced by a fresh H_2SO_4 solution (density 1.24 g cm^{-3}) and when the cell

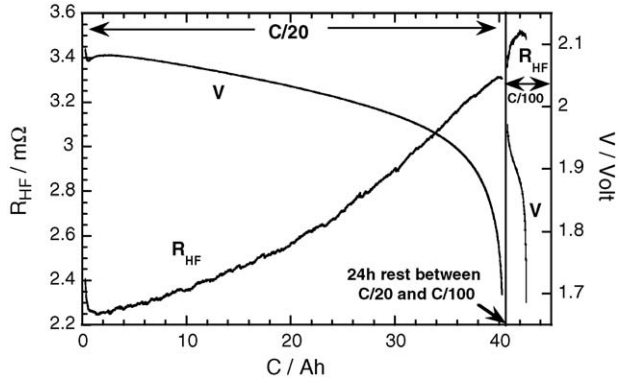

Fig. 5. Evolution of R_{HF} during a two-step discharge cycle ($C/20$ and $C/100$ after a 24 h rest).

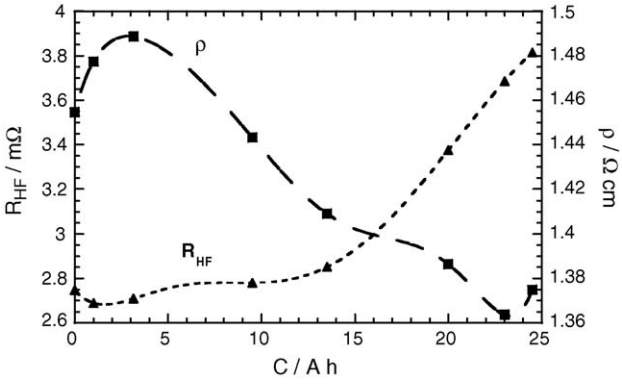

Fig. 6. Evolution of R_{HF} and ρ during a $C/100$ discharge.

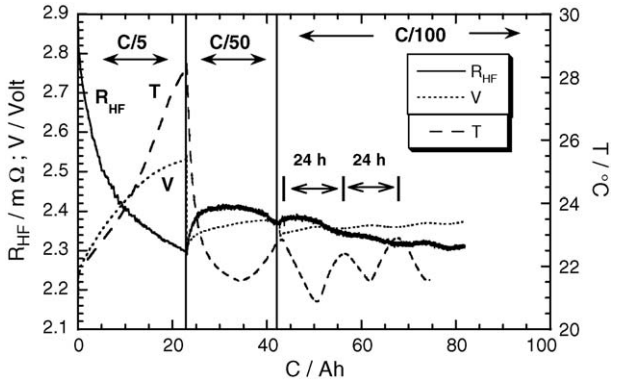

Fig. 7. Evolution of R_{HF}, V, and T during a combined charge at a rate of $C/5$, $C/50$, and $C/100$.

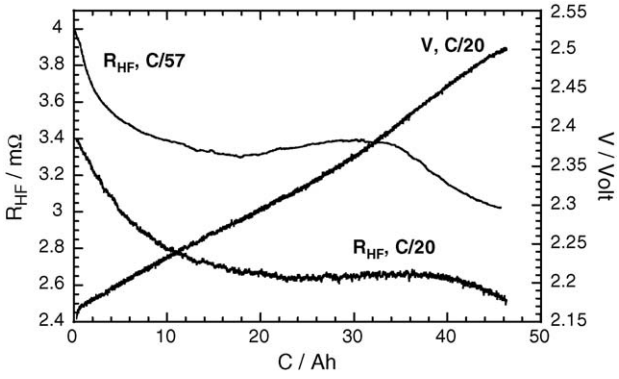

Fig. 8. Evolution of R_{HF} during the charge of the LAB cell at $C/20$ and $C/57$ rates and evolution of V at a $C/20$ charge rate.

was refilled with the previously exhausted electrolyte. Moreover, if the high value of R_{HF} at the end of a $C/100$ discharge was due to the bulk-electrolyte resistivity, the R_{HF} values of the positive and negative plates, which include the contribution of the bulk-electrolyte resistivity since the reference electrode was positioned above the plates, would have been close, which was not the case (Tables 2 and 3).

The electrolyte temperature, T, is another parameter potentially related to the R_{HF} values. Fig. 7 shows the concomitant evolution of V, R_{HF}, and T measured above the plates of a LAB cell during a combined $C/5$, $C/50$, and $C/100$ charge so as to evaluate the effect of the different rates on the electrolyte temperature. At a strong charge rate ($C/5$), a net temperature increase of about 6 °C was measured with a concomitant R_{HF} decrease of 0.5 mΩ, while at the low charge rates ($C/50$ and $C/100$), the electrolyte temperature simply tracked the room temperature with a very slight influence on the R_{HF} value. The relative variation of the electrolyte resistivity $\Delta\rho/\rho$ between 20 °C and 30 °C is about 1.6% per degree [14], so that a net increase of 6 °C corresponds to a decrease in R_{HF} of 0.28 mΩ if R_{HF} is supposed to be proportional to ρ. This could let imagine a large influence of the temperature on R_{HF}. However, a thorough examination of Fig. 7 shows that in the periodic temperature oscillation observed during the $C/100$-rate charge the R_{HF} variations were not induced by temperature variations. Indeed, between 56 Ah and 62 Ah of charged capacity, the 0.86 °C decrease in temperature would lead to a R_{HF} increase of 31.6 μΩ, much higher than the 3.6 μΩ measured. Fig. 8 shows the R_{HF} profile during a $C/20$ and a $C/57$ charge. In spite of expected temperature differences between the two rates, the R_{HF} values evolved in an almost "parallel" way, which confirms the minor effect of the electrolyte temperature on the measured R_{HF} values. The difference in the R_{HF} values (3.4 mΩ and 4.0 mΩ) at the beginning of the charge is due to the fact that the preceding discharges were not performed at the same rate. At both rates, R_{HF} decreased rapidly at the beginning of the charge because of the dissolution of the insulating $PbSO_4$ crystals, then R_{HF} remained almost constant before decreasing again at SOC higher than 80%, probably because the strong increase in dissolved gas production enhanced bubble ejection, hence decreasing the bubble screening effects.

Although R_{HF} was undoubtedly related to the SOC and also probably to the SOH of LABs, the results presented above show that it cannot afford the reliability necessary to a straightforward on-line diagnosis of the actual SOC; depending on the discharge profile, a given R_{HF} value can indicate different charge levels, as shown in Fig. 4. Overcoming this limitation may be possible by monitoring also the fluctuations of potential and electrolyte resistance by means of electrochemical noise measurements. Fig. 9 illustrates the typical behaviour of potential fluctuations, ΔV, measured at the LAB cell terminals at several stages of a LAB discharge at $C/100$. For a clearer reading, the linear potential drift due to the cell discharge was eliminated in the time records. The potential noise at different SOC values does not reveal elementary transients that could provide useful information on the discharge evolution. On the contrary, the R_{HF} fluctuations measured simultaneously in the same discharge conditions show easily discernable transients which were less numerous as the discharge went on, as seen in Fig. 10. These sudden R_{HF} decreases were induced by the detachment of gas bubbles formed during the preceding charge. Due to the fact that R_{HF} measurements encompass phenomena taking place both in the negative and positive plates, it is difficult to know whether hydrogen or oxygen bubbles were at the origin of the R_{HF} fluctuations: oxygen bubbles were produced on the positive electrode during the last charge, and also, hydrogen bubbles evolved on

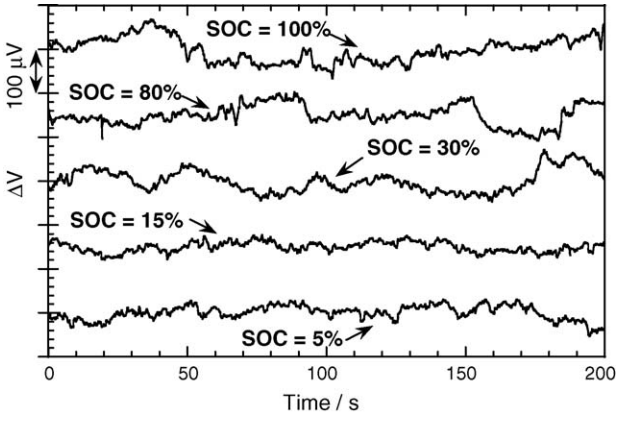

Fig. 9. Potential fluctuations, ΔV, after linear trend removal measured at the LAB terminals at different SOC during a $C/100$ discharge.

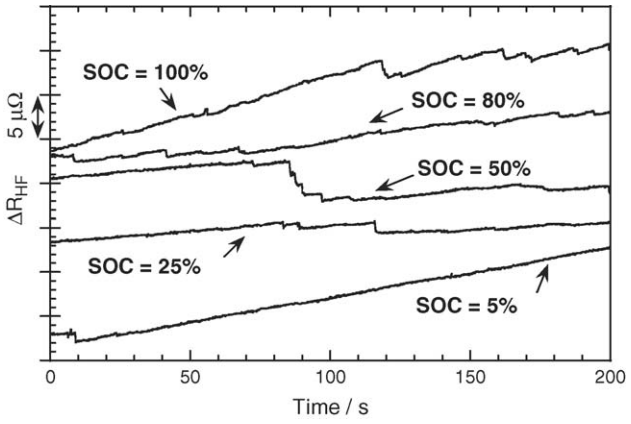

Fig. 10. R_{HF} fluctuations measured at different SOC during a *C*/100 discharge simultaneously with the potential fluctuations shown in Fig. 9.

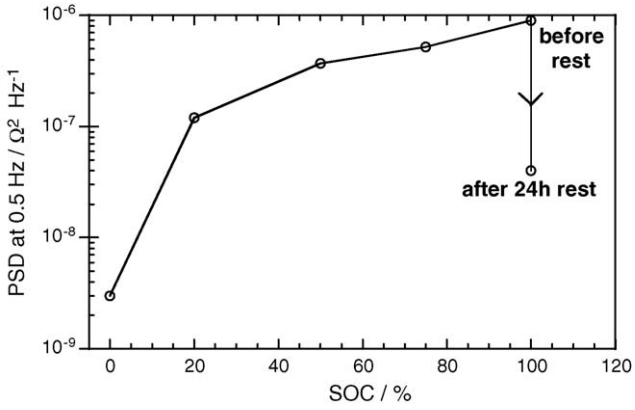

Fig. 12. Power spectral density at 0.5 Hz of the R_{HF} fluctuations measured at different SOC during a *C*/8 charge and presented in Fig. 11.

the negative electrode, which was overcharged before the positive electrode. The birth, growth, and departure of bubbles entail local changes in their screening effects that induce fluctuations in the electrolyte resistance around its mean value. This brings up the idea that if gas bubbles are already present before the final stage of the charge, their increasing density as the cell is charged would entail different noise signatures that could help in the evaluation of the SOC. Fig. 11 illustrates the R_{HF} fluctuations at different stages of a LAB charge at a high rate (*C*/8). At the beginning of the charge, when the LAB was still discharged, the R_{HF} signal was almost flat, even if some jumps of small amplitude (ca. 1 μΩ) could already be detected. As the charge went on, the curves became noisier due to stronger bubble evolution on the plates, especially above a SOC of 20%. It is interesting to note that the amplitude of the sudden R_{HF} decreases remained almost constant (ca. 10 μΩ), indicating that the mean size of the detaching bubbles did not increase with the SOC, certainly because it was controlled by geometrical parameters such as the distance between the plates. After a 24 h rest, the R_{HF} fluctuations measured at a zero current still showed sudden R_{HF} decreases of high amplitude (ca. 5 μΩ). On the contrary, the bubble departure rate seemed to monotonically increase during the charge. These results, although preliminary, offer an interesting perspective to monitor the SOC or SOH by means of an electrochemical noise-based parameter, like for instance the standard deviation or the power spectral density (PSD) at a given frequency of the R_{HF} fluctuations, or the mean time between two successive bubble departures during a few minutes of charge; when the SOC increases, the amount of gas produced during a given time increases, which could be detected by R_{HF} fluctuation measurements. As an example, Fig. 12 presents the amplitude of the PSD of the R_{HF} fluctuations shown in Fig. 11, calculated at a frequency of 0.5 Hz. The increase in the intensity of the gas evolution with SOC and the decrease after a 24 h rest are clearly monitored by the amplitude of the PSD.

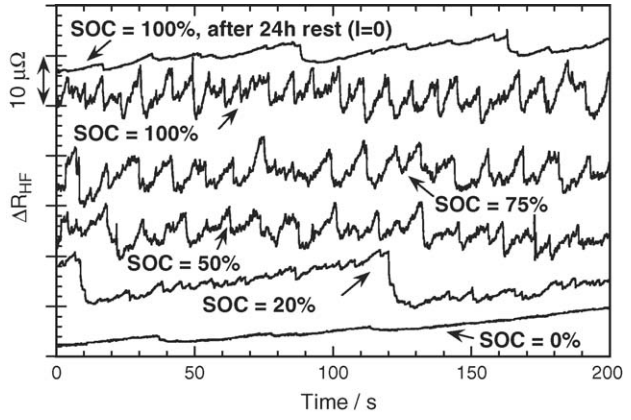

Fig. 11. R_{HF} fluctuations at different SOC during a *C*/8 charge.

4. Conclusions

The high-frequency resistance of 45 Ah flooded tubular LAB cells has been investigated with the aim of determining the origin of its variations with the cell SOC and evaluating the possibility of devising a reliable SOC indicator based on R_{HF} measurements.

While R_{HF} is independent of the charging or discharging current at the time it is measured, R_{HF} clearly varies with the SOC of the cell in a way that strongly depends on the charge or discharge regime, indicating that R_{HF} is a function of the history of the previous charges and discharges of the cell. Accordingly, the variations of the bulk-electrolyte conductivity, which is the commonly accepted explanation of the R_{HF} variations, could not explain the R_{HF} evolution with SOC in this work. The interpretation of the R_{HF} variations with SOC is based on the shape and size of the lead sulphate crystals deposited on the plates: at a high discharge rate, numerous small crystals partially block the pores of the active material, inducing a progressive R_{HF} increase since the beginning of the discharge with a relatively low final value of R_{HF}. On the contrary, at a low discharge rate, well-structured crystals need time to completely block the pores with the consequence to postpone the R_{HF} increase in the last third part of the discharge with a high final value of R_{HF}.

The results presented in the present paper show that, in spite of significant changes in the instantaneous R_{HF} value of fully charged and fully discharged LAB cells, this parameter is not suitable for being employed alone as a reliable SOC-monitoring

gauge, because most of the R_{HF} changes are concentrated at the final stage of the charge/discharge and also because of the strong dependence of the final R_{HF} value on the charge/discharge rate. However, coupling conventional R_{HF} measurements to the analysis of R_{HF} fluctuations, which detect the occurrence and the intensity of gas evolution, seems to be an interesting way to gather deeper information on the SOC and SOH evolution.

Acknowledgements

The authors would like to acknowledge the financial support of CEAC and ADEME (Convention No. 99-05-081).

References

[1] R.T. Barton, P.J. Mitchell, J. Power Sources 27 (1989) 287–295.
[2] M. Bayoumy, S. El-Hefnaw, O. Mahgoub, A. El-Tobshy, Sol. Energy Mater. Sol. Cells 35 (1994) 509–514.
[3] C. Armenta-Deu, Renewable Energy 4 (1994) 249–256.
[4] F. Huet, J. Power Sources 70 (1998) 59–69.
[5] S. Rodrigues, N. Munichandraiah, A.K. Shukla, J. Power Sources 87 (2000) 12–20.
[6] B. Hariprakash, S.K. Martha, A. Jaikumar, A.K. Shukla, J. Power Sources 137 (2004) 128–133.
[7] M. Thele, S. Buller, D.U. Sauer, R.W. De Doncker, E. Karden, J. Power Sources 144 (2005) 461–466.
[8] E. Karden, P. Shinn, P. Bostock, J. Cunningham, E. Schoultz, D. Kok, J. Power Sources 144 (2005) 505–512.
[9] N. Yahchouchi, Ph.D. Thesis, University, Paris 6, France, 1981.
[10] D.O. Feder, T.G. Croda, K.S. Champlin, S.J. McShane, M.J. Hlavac, J. Power Sources 40 (1992) 235–250.
[11] G.J. Markle, Proceedings of the INTELEC Conference, Washington, DC, 4–8 October, 1992, pp. 212–217.
[12] F. Huet, R.P. Nogueira, L. Torcheux, P. Lailler, J. Power Sources 113 (2003) 414–421.
[13] H. Blanke, O. Bohlen, S. Buller, R.W. De Doncker, B. Fricke, A. Hammouche, D. Linzen, M. Thele, D.U. Sauer, J. Power Sources 144 (2005) 418–425.
[14] H. Bode, Lead-Acid Batteries: The Electrochemical Society Series, John Wiley & Sons, New York, 1977.